JOURNAL OF CATALYSIS 60, 356–368 (1979)

Morphology of Pt–Rh Alloy Crystallites on Amorphous SiO_2[1]

M. CHEN, T. WANG, AND L. D. SCHMIDT

Department of Chemical Engineering and Materials Science, University of Minnesota, Minneapolis, Minnesota 55455

Received February 5, 1979; revised April 24, 1979

High-resolution scanning transmission electron microscopy is used to examine the structures of 20- to 200-Å-diameter Pt–Rh alloy particles on planar amorphous SiO_2 substrates following treatment in N_2 and air at one atmosphere and temperatures up to 1000°C. Heating in N_2 produces only alloy particles at all temperatures, while heating particles in air above 400°C produces a rhodium oxide layer around each particle. As temperature is increased above ~600°C the oxide appears to migrate onto the SiO_2 substrate to form a thin oxide layer surrounding the metal core. The oxide is identified as Rh_2O_3 by electron diffraction, and dark field imaging confirms the morphology postulated. Pure Rh particles are completely oxidized by 600°C and remain stable to at least 1000°C. Continuous 10-Å-thick films of Rh or Pt–Rh cannot be broken up into particles below ~700°C by heating in air because the oxide film is stable and adheres strongly to the SiO_2. This alloy system is quite different than Pt–Pd in that the oxide forms as a thin Rh_2O_3 layer around each particle for Rh, while for Pd, a PdO crystallite nucleates at the side of the metal crystallites. Both oxides adhere strongly to SiO_2, but the nucleation and growth of Rh_2O_3 is evidently much different than PdO.

INTRODUCTION

Supported alloy and multimetal catalysts are finding increasing usage because their reactivity, selectivity, and stability can be easily controlled by altering composition and preparation procedures (*1*, *2*). The Pt–Pd–Rh system has wide use in industrial catalysts, especially in the automotive converter where it catalyzes several reactions under widely variable and transient conditions of temperature and composition.

While single metals which do not form compounds with reactants (mainly Pt) have been shown to exist as small crystallites, the morphology and composition of multimetal catalysts can be much more complex. Each species generally has a different ability to form compounds, and the metals and compounds have different mobilities and interfacial properties between phases.

We have previously reported studies of Pt (*3*) and of Pt–Pd alloys (*4*) on amorphous SiO_2 using high-resolution scanning transmission electron microscopy (STEM), electron diffraction, and X-ray microanalysis to examine the effects of oxidizing and reducing atmospheres on particle size, morphology, and composition. We showed that Pt exists as single crystal or twinned particles in N_2 or air, but that in air particles grew much more rapidly below 700°C and evaporated as PtO_2 at higher temperatures. Pt–Pd alloys behaved much as Pt in N_2, but in air PdO crystallites nucleated at the edge of metal particles above ~400°C. At ~700°C PdO decomposed to

[1] This work partially supported by NSF under Grant No. ENG75-01918 and by PRF under Grant No. 10864-AC-7.

0021-9517/79/150356-13$02.00/0

TABLE 1

Properties of Metals and Oxides[a]

Metal	Melting point (°C)	Vapor pressure at 800°C (Torr)	Solid oxide	Crystal structure	Decomposition temperature (°C)	Vapor pressure of oxide at 800°C (Torr)
Pt	1769	9.1×10^{-17}	PtO_2	Hexagonal	280, 450	1.2×10^{-5}
Rh	1966	2.9×10^{-17}	Rh_2O_3	Rhombic	990, 1100	5.8×10^{-6}
			RhO_2	Tetragonal	1030, 1400	
Pd	1552	1.2×10^{-9}	PdO	Tetragonal	700	Negligible

[a] Date from Ref. (*5*).

metal, but X-ray microanalysis and micrographs showed that distinct Pt-rich and Pd-rich crystals remained. Room temperature hydrogen reduction of PdO also produced distinct crystallites of the separated metals.

In this paper we examine the effects of heating Pt–Rh crystallites on SiO_2 in air and in N_2. We shall show that their behavior is quite different from Pt–Pd alloys (*4*) even though in both cases one species readily forms an oxide. Evidently, nucleation and growth processes of the phases are quite different.

Both Pt–Rh and Pt–Pd form solid solutions at all compositions and temperatures. As shown in Table 1, Rh forms two stable oxides, Rh_2O_3 and RhO_2, which are stable to >1000°C in air at 1 atm (*5*). Both Rh and its oxides have much lower vapor pressures than Pt or its oxides. Palladium forms solid PdO which is stable to ~700°C, and PdO has a lower vapor pressure than either Pt, Rh, or their oxides (*5*).

Because of the importance of Pt–Rh alloy catalysts in NH_3 oxidation to NO and in NO removal in the automotive converter, there have been extensive kinetic studies on these surfaces (*6*, *7*). However only limited characterization of Rh or Pt–Rh crystallites has been reported (*8–10*). Recently Fiedorow *et al.* (*9*) compared sintering rates of Pt, Rh, and Ir on Al_2O_3 in H_2 and O_2 atmospheres. In O_2 Rh was found to be more stable than Pt while in H_2, Pt was more stable.

EXPERIMENTAL

Apparatus and procedures have been described in detail previously (*3*, *4*). Experiments consisted of depositing 5- to 20-Å films of metals onto planar amorphous SiO_2 substrates ~500 Å thick, heating these films in flowing air or N_2 to form particles, and examining them in a JEOL JEM100C scanning transmission electron microscope.

Silica substrates were prepared by chemical etching and argon ion micromilling single crystal Si discs which were then oxidized in air at ~1200°C. This produces a thin uniform layer of amorphous SiO_2 in which no contamination was detectable by electron diffraction, scanning Auger microanalysis, or X-ray microanalysis. These SiO_2 substrates are self-supporting and are not exposed to liquids at any time following their preparation. Since the SiO_2 is amorphous, it is relatively uniform and exhibits no diffraction contrast or substrate diffraction lines which would interfere with diffraction analysis of particles on its surface.

Metal films were vacuum deposited sequentially to thicknesses of ~10 Å with compositions believed to be accurate to within ±5%. Films were broken up into 10- to 20-Å crystallites by heating in vacuum or in N_2. For Pt or Pt–Pd, 300°C

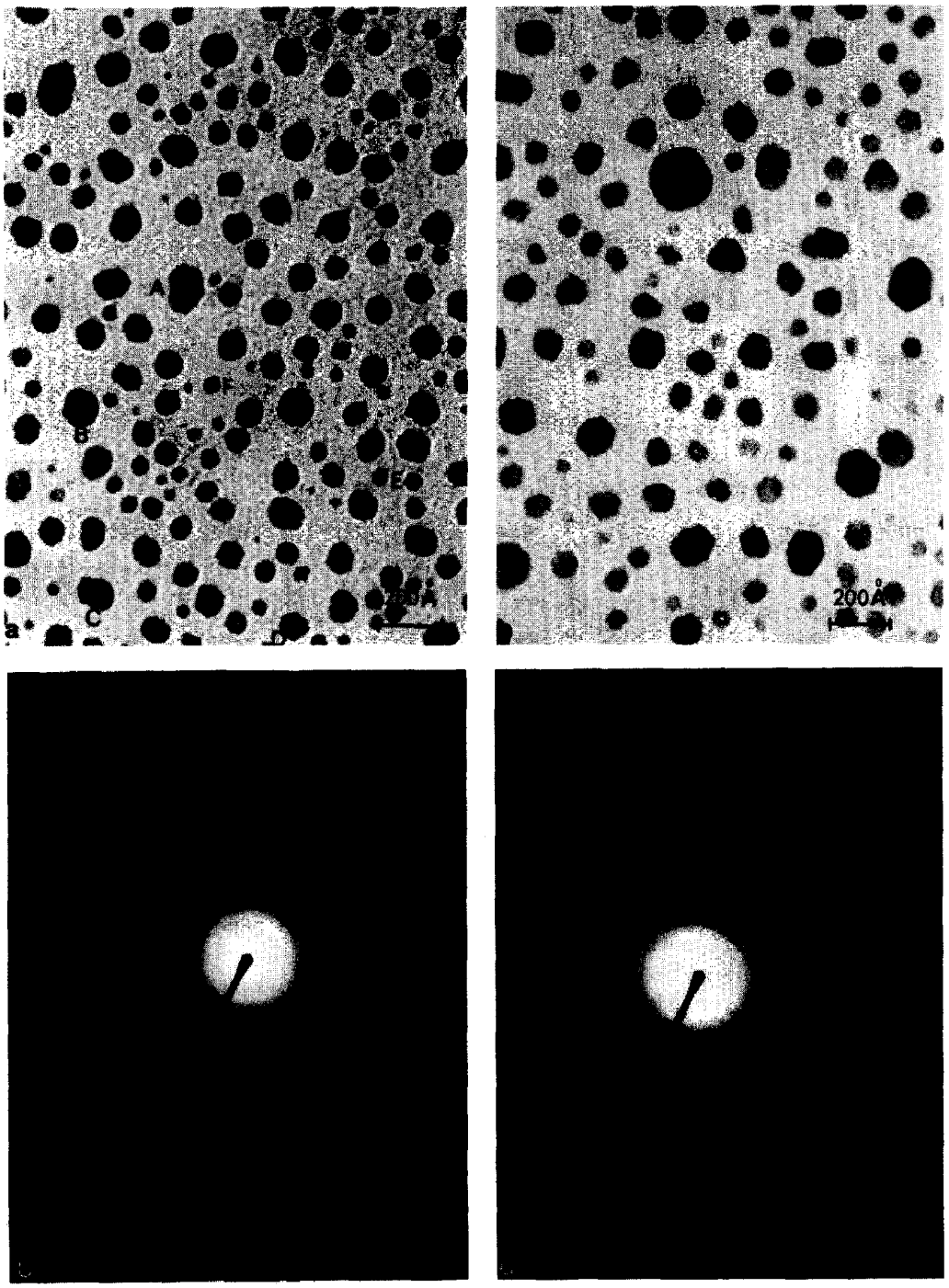

FIG. 1. Transmission electron micrographs showing the morphologies of Pt–Rh alloy particles formed by heating ~20-Å films of a Pt–56% Rh on SiO_2 in N_2 for 1 hr at (a) 650°C and (b) 800°C. (c) The electron diffraction pattern of (a) showing the crystallites are fcc solid solution, and (d) the electron diffraction pattern of the specimen shown in Fig. 2d which is only Rh_2O_3. The diffuse rings of SiO_2 near the origin are the only diffraction features observed except for metal and Rh_2O_3.

was sufficient for breakup, but for Pt–Rh continuous films remained until ~500°C.

Specimens were heated in flowing gases at flow velocities of ~5 cm/sec in a quartz tube furnace. Specimens were transferred repeatedly between oven and microscope so that sequential micrographs of the same region of a specimen could be examined as functions of temperature, time, or gas. No evidence of contamination during transfer or microscopic examination was noted.

RESULTS

Alloys

Heating in N_2. Figures 1a and b show micrographs of a 56% Rh alloy which had been heated in N_2 to 650 and 800°C, respectively. These micrographs appear qualitatively similar to those for Pt or Pt–Pd alloys following similar treatment, except that particles appear to be slightly more irregular (fewer perfect polyhedra) and may possess more single and multiple twins than for pure Pt. Electron diffraction pattern (Fig. 1c) showed only the sharp rings of a randomly oriented fcc metal in addition to the diffuse rings of amorphous SiO_2.

Heating crystallites in air. The specimen shown in Fig. 1a which had been heated in N_2 at 650°C to form alloy crystallites of ~70 Å diameter was then heated in air at successively higher temperatures. Figure 2 shows micrographs of this specimen following 1 hr heat treatments at temperatures of 310, 400, 600, 690, 750, and 850°C. At 310 and 400°C little change is produced by heating in air although at 400°C the edges of particles appear to become slightly "fuzzier" as shown in Fig. 2b.

However, after heating to 600°C (Fig. 2c), a lower contrast region 10 to 20 Å wide has begun to form around all particles. After heating to 690°C this region has broadened to 20 to 30 Å, and it continues to grow at 750°C as shown in Fig. 2e. At 850°C (Fig. 2f), the Pt has presumably evaporated as PtO_2, leaving a few large particles of rhodium oxide.

This morphology is accompanied by the appearance of Rh_2O_3 in electron diffraction. Figure 1d shows the diffraction pattern of the specimen shown in Fig. 2d, and lines characteristic of fcc metal and the orthorhombic Rh_2O_3 are noted. No lines of RhO_2 or any other oxides have been identified in this study, and we conclude that Rh_2O_3 is the only stable crystalline oxide formed under these conditions.

Examination of Fig. 2 also shows that, upon heating in air to successively higher temperatures, all particles appear to *increase in diameter.* This is not due to sintering because the temperatures are lower than those used in previous treatment in N_2 all particles appear to grow in contrast to the situation required by the Ostwald ripening mechanism and no particles more as required by the coalescence mechanism. Rather, it is caused by particles swelling and spreading over the substrate as Rh_2O_3 forms.

The existence of high-contrast nuclei at the center of most low-contrast particles is consistent with the interpretation of Pt at the center and thin Rh_2O_3 at the edges. The atomic scattering factor of Pt is 1.73 times that of Rh, and there is a density decrease of 34% between Rh and Rh_2O_3.

The morphology of metal and Rh_2O_3 was confirmed by dark field imaging of a specimen heated to 650°C in air for 1 hr. Figure 3a shows the bright field image of a region while Figs. 3b and c show the dark field images of metal and oxide, respectively. These were obtained with a portion of the {200} diffraction ring of fcc and the most intense group of lines of Rh_2O_3. The aperture subtended only a small portion of the diffraction ring and therefore only those crystallites with proper orientation "light up." Only portions of the Rh_2O_3 or Pt are therefore observed in dark field images. However these micrographs confirm the conclusion that the dark field image of the

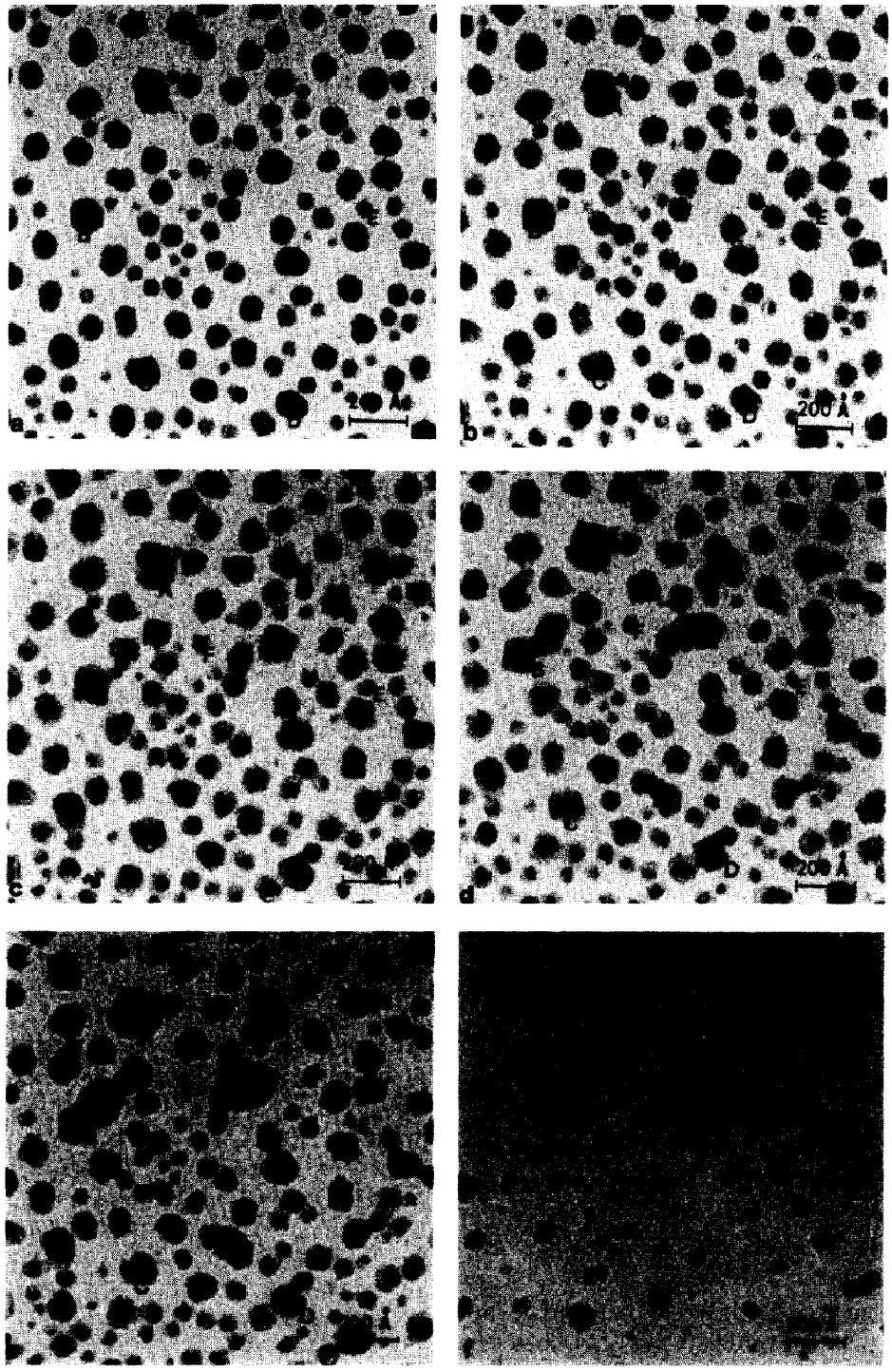

FIG. 2. Micrographs of 56% Rh alloy on amorphous SiO_2 after heating in air for 1 hr at temperatures of (a) 310°C, (b) 400°C, (c) 600°C, (d) 690°C, (e) 750°C, and (f) 850°C. Several particles are indicated in each micrograph, and sizes of these particles are plotted in Fig. 7.

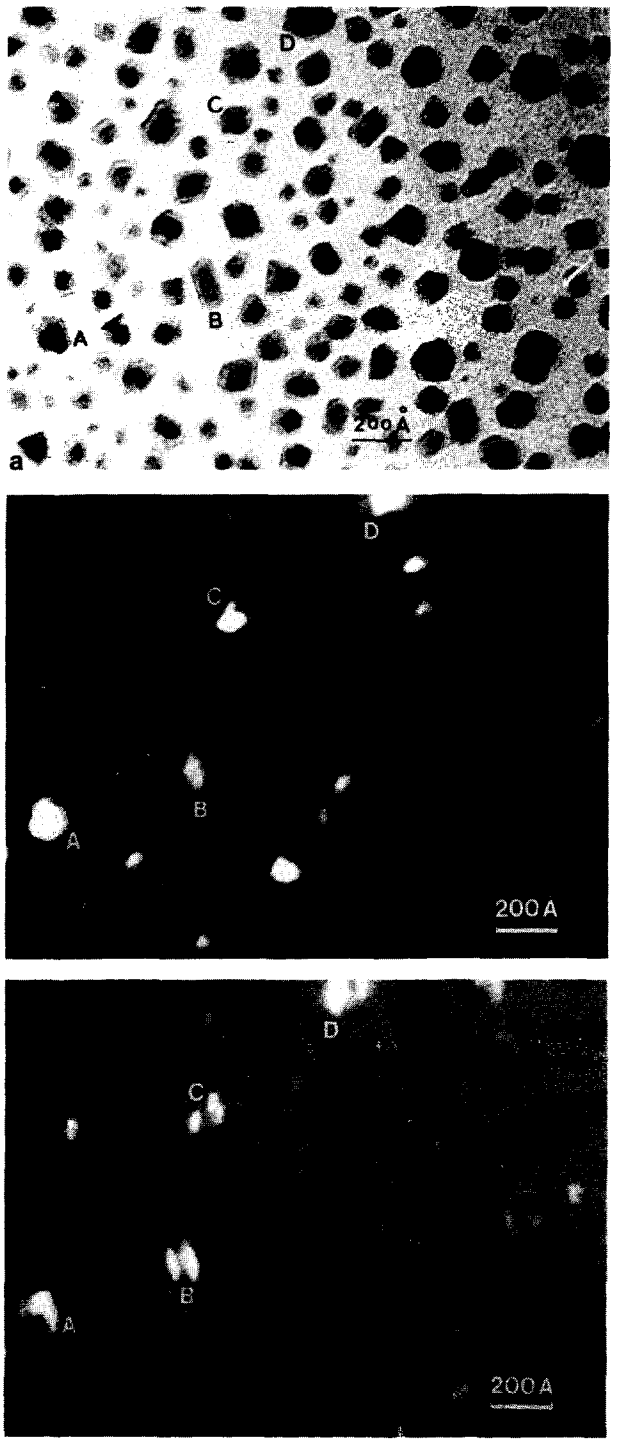

FIG. 3. Micrographs illustrating partial oxidation of 56% Rh alloy. Specimens were heated to 650°C in air for 1 hr. (a) The bright field image, (b) the dark field image of metal, and (c) the dark field image of Rh_2O_3.

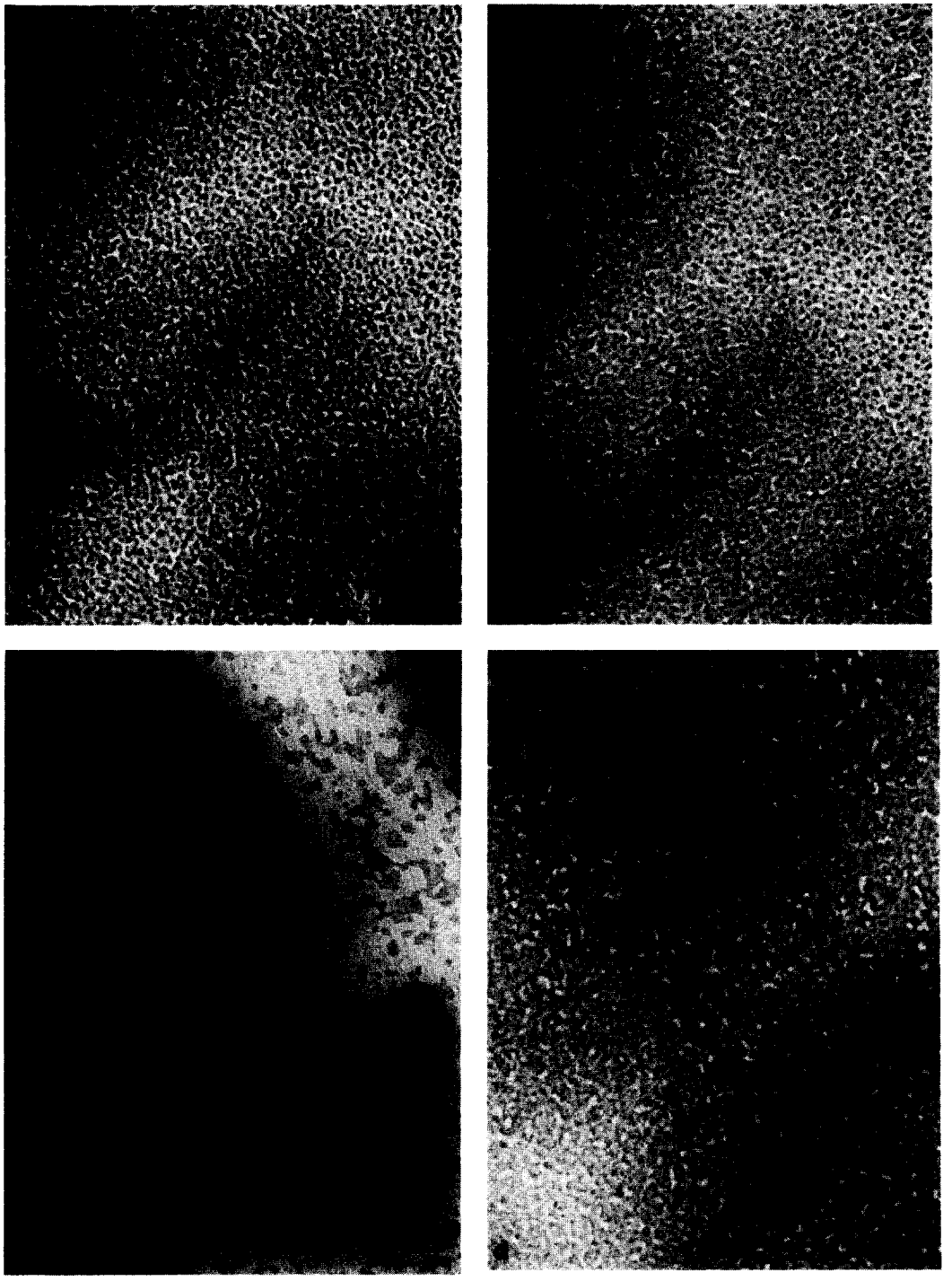

FIG. 4. Micrographs of a 75% Rh alloy film following heat treatments in air for 1 hr at (a) 300°C, (b) 700°C, and (c) 800°C. This shows that the Rh film breaks up only partially even at ~800°C, but that Pt crystallites (~50 Å dark regions) form readily. (d) The micrograph of a pure Rh specimen following heating in air for 1 hr at 700°C.

metal coincides with the cores of particles while the dark field images of Rh_2O_3 coincides with their periphery.

We also note that all sequential micrographs show that no particle motion had occurred to distances greater than a fraction of particle diameters. This confirms the previous observation for Pt and Pt–Pd on SiO_2 (*3*, *4*) that atomic migration rather than particle coalescence is the sole mechanism of particle sintering.

Following heating at 850°C, Fig. 2f shows that considerable metal loss has occurred, probably through evaporation. However the particles remaining can be identified as residues of particles observed at lower temperatures (Fig. 2e).

Heating alloy films in air. It was impossible to break up Pt–Rh films by heating in air below ~700°C. Figures 4a and b show micrographs of a 75% Rh alloy film following heat treatments for 1 hr at 300 and 700°C, respectively. Micrographs are essentially identical and show an almost continuous film of Rh_2O_3 with darker crystallites of metal. Electron diffraction confirms the existence of both phases. Evidently the film oxidizes rapidly below 300°C to form a film which is quite stable toward breakup.

At 800°C the film breaks up to form large 200- to 400-Å particles as shown in Fig. 4c. Diffraction contrast in the micrograph shows that the particles are all polycrystalline, and electron diffraction indicates only Rh_2O_3. All Pt should have evaporated at this temperature and as discussed later this implies Pt evaporation is inhibited in the alloy or that Rh remains. Results in the next section show that Rh is completely oxidized by 600°C.

Rhodium

Heating Rh films in N_2 produced crystallites whose morphology and sintering characteristics were indistinguishable in size and shape from Pt at comparable initial film thicknesses. As just noted, films heated in air remained continuous without breakup into crystallites to ~800°C.

The effect of heating pure Rh in air was therefore examined by first preparing Rh crystallites by heating Rh films to 650°C in N_2. Oxidation by traces of O_2 or H_2O was avoided by adding a few percent of H_2 to the N_2 stream. Figure 5a shows the micrograph of a Rh film after this treatment. Particles have an average size of 60 Å. Figures 5b–h show micrographs of this region after heating in air for 1 hr at temperatures of 320, 410, 500, 620, 695, 810, and 870°C. All particles begin to increase in diameter even at 320, and by 500°C all metal lines have disappeared and only lines of Rh_2O_3 remain.

The formation of oxide can be followed from the shrinking of twinned regions in metal particles which initially have twins. As noted in the micrographs, all particles exhibiting single or multiple twins in the metal (because of diffraction contrast) exhibit a reduction in the twinned area upon heating in air, and twins disappear by 500°C.

DISCUSSION

Morphology Produced by Heating in Air

When the Pt–Rh alloy is heated in air, Rh_2O_3 is observed to form more or less uniformly around the edge of each metal particle. The location of oxide at the edges of particles is inferred from the lower contrast, the irregularity of shapes compared to metal, and dark field microscopy (Fig. 3).

Figure 6 shows a plot of the diameter of individual particles of pure Rh versus temperature produced by heating in air. and Fig. 7 shows diameters of particle (solid lines) and metal core (dashed lines) for the Rh alloy. Data were obtained from micrographs shown in Figs. 5 and 2, respectively. Diameters were measured by averaging sizes of individual particles mea-

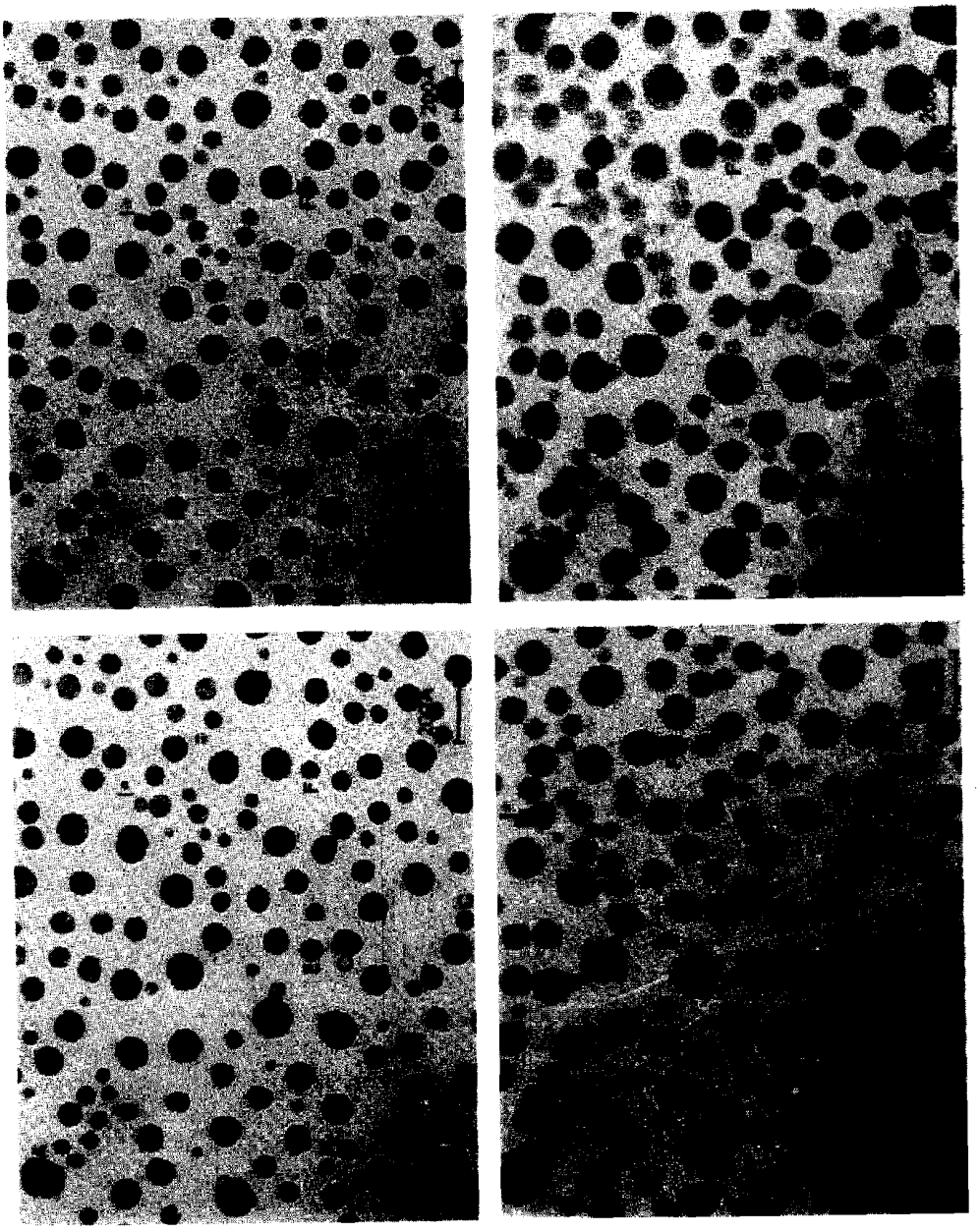

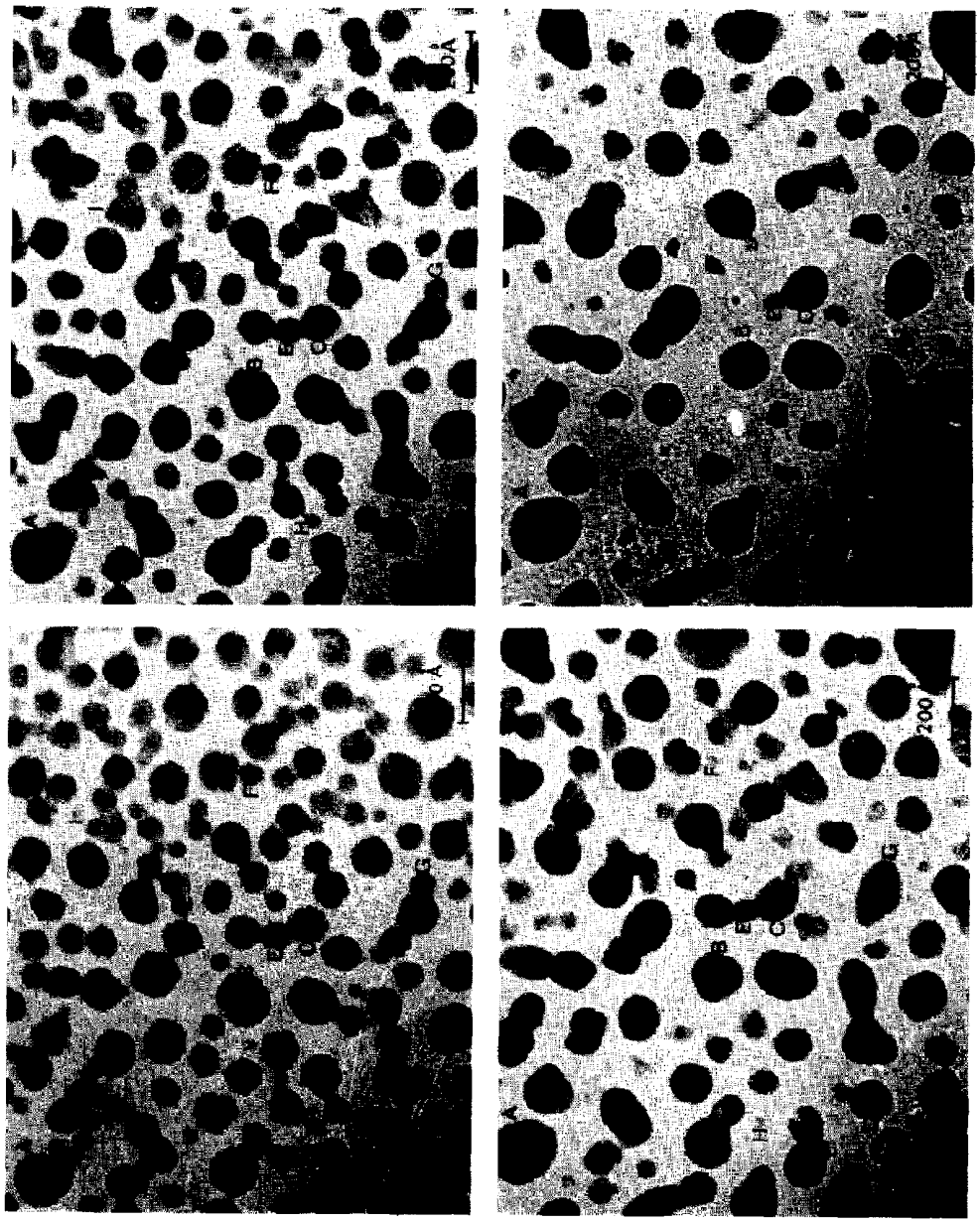

FIG. 5. Transmission electron micrographs showing the morphologies of Rh_2O_3 and metal particles formed by heating pure Rh on SiO_2 for 1 hr in (a) N_2 at 650°C and then in air at successively higher temperatures of (b) 320°C, (c) 410°C, (d) 500°C, (e) 620°C, (f) 695°C, (g) 810°C, and (h) 870°C. Several individual particles are indicated in each figure, and diameters are plotted in Fig. 6.

sured in two directions. While only a small number of particles were analyzed (because many particles combine at low temperature), we attempted to obtain a representative distribution of initial sizes. The metal diameter was measured from the size of the higher contrast core region at the center of each particle.

The diameters of all particles clearly increase as the temperature is increased up to ~500°C; for the particles in Figs. 6 and 7 the average diameter increases were 40 and 33% for Rh and alloy, respectively. Above 500°C all particles with diameters less than 100 Å begin to shrink while those above 100 Å continue to grow.

For Rh, of the particles with initial diameters less than 80 Å, two disappeared before 810°C, two more by 870°C, and

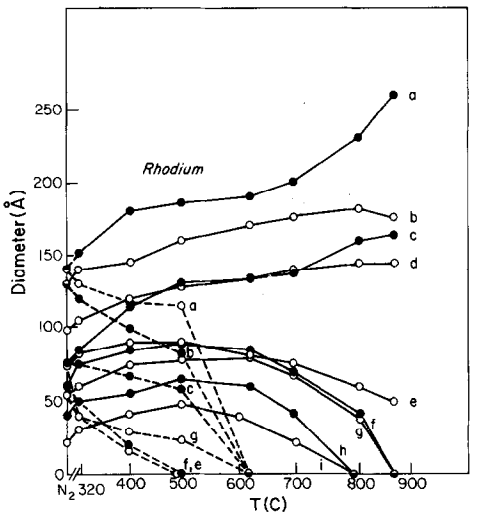

FIG. 6. Plot of the diameter of individual particles (data from particles labeled in Fig. 5) of pure Rh versus temperature produced by heating first in N_2 and then air at the temperatures shown. Diameters were measured by averaging sizes of each particle measured in two dimensions. Solid lines show overall diameters of particle while dashed lines show diameter of higher contrast metal cores. The metal core is observed to disappear completely by 600°C. A uniform increase in apparent diameter occurs on all particles below ~500°C because of density decrease and spreading over the surface. Above this temperature large particles grow and small ones shrink as predicted by the atomic diffusion model of sintering.

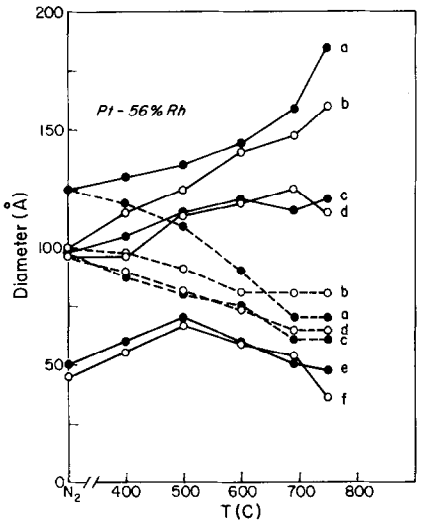

FIG. 7. Plot of the diameter of individual particles (data from particles labeled in Fig. 2) of 56% Rh alloy versus temperature produced by heating first in N_2 and then in air at temperatures shown. Solid and dashed lines show diameters of particle and metal core, respectively.

only one (labeled c) grew. This is a clear illustration of sintering by the atomic diffusion or Ostwald Ripening mechanism with the critical size for this initial distribution being ~100 Å.

For the alloy the behavior is qualitatively similar, although the situation is complicated by the presence of the metal core (presumably mostly Pt). The metal cores shrink continuously but do not disappear even at 850°C.

For pure Pt crystallites on SiO_2 all metal would have disappeared completely by this temperature if heated in air because of loss through volatile PtO_2. It appears, therefore, that in Pt–Rh alloys the presence of Rh_2O_3 strongly inhibits evaporation of Pt. The core would not be expected to

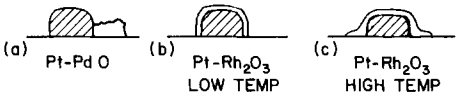

FIG. 8. Schematic diagrams of the morphologies of Pt–Pd and Pt–Rh alloy on SiO_2 sintered in air: (a) Pt–Pd alloys, (b) Pt–Rh low temperature oxidation, and (c) Pt–Rh high temperature oxidation.

contain Rh metal since no metal remains above 500°C when starting with pure Rh. Inhibited Pt evaporation was also noted in the Pt–Pd alloy, and the cause suggested was the reduced volatility of Pt because it may be covered by a PdO layer. A similar mechanism may apply in this system, and the Rh_2O_3 appears even more likely to exist as a film over the Pt core.

We can estimate the change in the height to diameter ratio h/d of Rh which accompanies oxidation by assuming no change in amount of Rh (both Rh and Rh_2O_3 have negligible vapor pressure below 600°C). The average diameter of particles shown in Fig. 6 increases by 35% between the metal and the oxide at 500°C. Much of this can be attributed to a density change between Rh and Rh_2O_3 which corresponds to a volume increase of 82% upon formation of Rh_2O_3. However, if the particles swelled with no change in shape, the diameter should increase only by 22% versus the observed 35%. The results can be best fit by assuming that particles *retain their original height* as they expand during oxidation. So that, as for Pd, particles spread over the SiO_2 upon oxidation. Above 600°C, growth is even more pronounced, although spreading on the SiO_2 cannot be distinguished from Ostwald ripening at high temperatures.

Morphology of Pt–Rh_2O_3 and Comparison between Pt–Rh and Pt–Pd Alloys

The morphologies we observe here upon heating in air are quite different from those reported previously for Pt–Pd alloys (*4*). In the two sets of experiments, identical conditions were used, as were metal and substrate preparation procedures.

With Pt–Pd the oxide invariably nucleated either as a single particle at the side of the metal crystallite (Fig. 8a), formed a particle not in contact with a metal particle, or several metal and oxide particles fused together. The oxidation appeared to be complete by 600°C, and the oxide particles did not change shape until ~700°C where they began decomposing back to Pt metal. We estimated the height h of oxide particles from the increase in diameter d of crystallites, and found that the h remained approximately constant while h/d decreased upon oxidation.

With Pt–Rh, however, the oxide first forms as a skin more or less uniformly around each particle. Whether oxide forms on top of (or below) the metal particle cannot be determined from shadow imaging alone, although the dark field micrographs (Fig. 3) indicate that oxide crystals overlap metal crystals. Therefore, we suggest that the oxide forms a skin over the metal cores as sketched in Fig. 8b. The particles continue to grow parallel to the surface as the temperature is increased, and it appears that Rh_2O_3 migrates out onto the SiO_2 substrate upon heating. However, our observed contrast and the calculated amount of Rh strongly argues that all Rh and Rh_2O_3 particles have heights which are appreciable fractions of their diameters and are not monolayer films.

The thermodynamic properties of Pd and Rh, summarized in Table 1, give some suggestions for the observed differences in morphologies. Both form stable oxides in O_2, and PdO decomposes at ~700°C while Rh_2O_3 decomposes only above 1000°C (higher than temperatures used here). The major difference between Pd and Rh must be in the diffusion coefficients of their oxides or in oxide nucleation properties. Little data exist on diffusion coefficients of these metals, but, since Rh has the highest melting point, it might be expected to have the lowest diffusion coefficient. Surface diffusion and diffusion through oxides could of course be important in the observed differences between Rh and Pd.

We argued previously that PdO probably had better adhesion (lower interfacial energy) to SiO_2 than to Pt because the PdO particles spread out on the SiO_2 and be-

cause distinct Pt and PdO particles formed. The same argument cannot be made as strongly here because Rh_2O_3 particles never separate from Pt. However, Rh_2O_3 particles do have lower h/d ratios than do metal particles.

SUMMARY

Rh_2O_3 grows as a skin over Pt–Rh alloy crystallites upon heating in air, while for Pt–Pd distinct Pt and PdO particles are observed. Thus, these alloy catalysts should have quite different morphologies upon heating in air. Distinct Pt and Pd particles remain following H_2 reduction, while Rh should remain within the original particle. Therefore, one would expect that Pt–Rh alloy surfaces should become Rh-rich by oxidation–reduction treatment, while Pt–Pd alloys may have particles of both Pt and Pd.

We have not examined Pt–Rh metal compositions much different than a 1:1 atomic ratio. For Pt–Pd we observed quite different temperatures for formation and breakup of the oxide with composition. However, no corresponding effects are anticipated here because Rh_2O_3 forms immediately at 320°C while higher temperatures are required to form PdO. Also, PdO decomposes at 700°C while Rh_2O_3 is much more stable. The stability of Rh_2O_3 films toward sintering suggests that Rh catalysts in this form should retain very high surface areas under rather extreme conditions.

Of course, these techniques cannot detect monolayer enrichment of one metal. However, calculations of measurements of surface excesses in these alloy systems would appear from these results to have little obvious relation to the structure and surface composition of small alloy catalyst crystallites because they ignore the influence of morphology changes. As with Pd–Pd, cycling in temperature and gas composition should have marked effects on catalyst structure and composition.

REFERENCES

1. Wynblatt, P., and Gjostein, N. A., *Prog. Solid State Chem.* **9**, 21 (1975).
2. Wynblatt, P., and Ahn, T. M., "Materials Science Research, Vol. 10, Sintering and Catalysis," p. 83. Plenum Press, New York, 1975.
3. Chen, M., and Schmidt, L. D., *J. Catal.* **55**, 348 (1978).
4. Chen, M., and Schmidt, L. D., *J. Catal.*, **56**, 198 (1979).
5. Samsonv, G. V. (ed.), Turton, C. C. N., and Turton, T. I. (transl.) "The Oxide Handbook," pp. 217, 397. Plenum, New York, 1973.
6. Schlatter, J. C., and Taylor, K. C., *J. Catal.* **49**, 42 (1977).
7. Blasin *et al.*, *J. Catal.* **54**, 1201 (1978).
8. Yates, D. J. C., and Sinfelt, J. H., *J. Catal.* **8**, 348 (1967).
9. Fiedorow, R. M. J., Chahov, B. S., and Wanke, S. E., *J. Catal.* **51**, 193 (1978).
10. Prestridge, E. B., and Yates, D. J. C., Norelco, Rep. Vol. 18, No. 2, 39 (1971).